

# Experimental Snap-through Boundaries for Acoustically Excited, Thermally Buckled Plates

by K.D. Murphy, L.N. Virgin and S.A. Rizzi

**ABSTRACT**—This paper presents some recent experimental results on the dynamic snap-through behavior of a clamped, rectangular plate subject to thermal loading and intense acoustic excitation. The likelihood of snap-through oscillations is characterized in terms of boundaries separating regions of snap-through and no snap-through in the parameter space. Two scenarios are considered. First, using tonal inputs, the regions of snap-through are mapped in the sound pressure level—input frequency domain ((SPL,  $\omega$ ) plane). Second, random acoustic inputs are used, and the effect of varying the overall sound pressure level and frequency bandwidth are investigated ((SPL,  $\omega_{center} + \overline{\omega}$ ) plane). Several nonlinear characteristics are evident and discussed.

## Introduction

There are a number of circumstances where a slender structure, subject to a combination of axial and lateral loading, can exhibit snap-through behavior.<sup>1-5</sup> In a static context, buckling is usually accompanied by the appearance of multiple equilibria: the underlying potential energy function has a number of locally distinct minima,<sup>6</sup> and large perturbations may cause the system to “snap” to an alternate equilibrium configuration. In the dynamic context, lateral excitation may cause intermittent or persistent snap-through where the system now oscillates about, and between, the multiple equilibria.

From a practical point of view, these large amplitude, thoroughly nonlinear oscillations are detrimental to the integrity of the structure. Snap-through produces large changes in curvature over short time intervals, which increases wear and greatly reduces fatigue life. In extreme cases, catastrophic failure may result. As such, it would be useful to know under what circumstances snap-through is likely to occur.

It is the goal of this study to experimentally determine the parameters which result in snap-through oscillations for both deterministic and random inputs. To accomplish this, two sets of experimental results are presented. The first focuses on the initiation of snap-through using narrow band (tonal) acoustic inputs. The boundary separating regions of snap-through and no snap-through are mapped in the sound

pressure level-frequency plane. The second uses random acoustic excitation to consider the effect of frequency bandwidth on initiation of snap-through.

## Experiment Description

Figure 1 shows a schematic of the thermal acoustic fatigue apparatus (TAFE) at the NASA Langley Research Center. TAFE is a progressive wave tube facility used to subject plate structures to combined thermal and acoustic loads. A detailed description of the TAFE facility is provided in Ref. 7.

The acoustic waves, generated by two air modulators, propagate through an exponential horn to a 1.83 m  $\times$  1.83 m  $\times$  0.305 m test section, which leads to an anechoic termination. Within the test section, test specimens are mounted on the side wall and thus are subject to a grazing acoustic excitation. The system is capable of generating overall sound pressure levels between 125 dB and 165 dB. Furthermore, the frequencies may be either sinusoidal or broadband in a range of 40–500 Hz.

Thermal loads are provided by a set of 10 quartz lamp banks situated directly across the test section from the plate. The lamps can provide a maximum heat flux of 511 kJ/(m<sup>2</sup> s). A low-mass airflow is also used to minimize the effects of natural convection.

The frame was designed for a series of acoustic-thermal tests and is described in Refs. 8 and 9. The objective is to prevent thermal expansion of the frame so that the plate, as it expands thermally, will experience in-plane compression and eventually buckle. To accomplish this, insulating material is used to minimize heat conduction to the frame from both the plate and the test section. In addition, a water-cooled channel is welded to the frame to provide continuous cooling.

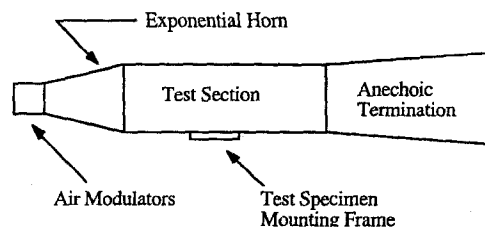


Fig. 1—An overhead schematic of the thermal acoustic fatigue apparatus (TAFE) at the NASA Langley Research Center and the plate mounting system

K.D. Murphy is Assistant Professor, Department of Engineering Mechanics, University of Nebraska, Lincoln, NE 68588-0347. L.N. Virgin is Associate Professor, Department of Mechanical Engineering, Duke University, Durham, NC 27708-0300. S.A. Rizzi is Research Engineer, NASA Langley Research Center, Structural Acoustics Branch, Hampton, VA 23681-0001.

The plate under consideration had dimensions  $0.381 \text{ m} \times 0.305 \text{ m} \times 1.58 \text{ mm}$  (aspect ratio =  $L_x/L_y = 1.25$ ) and is made of AISI 321 stainless steel. Based on the frequency response function, the first natural frequency is experimentally determined to be 111 Hz. Also, using the techniques described in Ref. 8, the critical temperature (above ambient) for the flat plate with experimental boundary conditions is  $\Delta T_{cr} = 11.6^\circ\text{C}$ .

Time series data are acquired using a high-temperature strain gage at  $(x, y) = (0.22 \text{ m}, 0.14 \text{ m})$  as measured from the lower left corner of the plate. This strain gage measures the  $y$ -direction strain (perpendicular to the direction of acoustic wave propagation). The strain gage circuit was zeroed after the plate was clamped into the frame. Consequently, all data are measured relative to the nonzero static equilibrium plus any additional deformation which resulted from the clamping procedure. Strain gage data are recorded using a workstation-based acquisition system. The sampling rate is set at 32,768 samples/s. Measurements are DC coupled in order to record the strains at the various equilibrium positions. The plate is also outfitted with several thermocouples to monitor the temperature and thereby ensure a uniform temperature distribution.

### Static Considerations

It is well established that the location and stability of the system's equilibria are dictated by the strain energy function.<sup>6</sup> For simplicity, assume the deflection of the system is given by a single generalized coordinate,  $q$ . Using some suitable nondimensionalization, the (strain) potential energy function for an axially loaded, slender structure in the initial postbuckled range takes the form

$$V(q) = q^4 - \lambda q^2 \quad (1)$$

where  $\lambda$  represents a control parameter, e.g., the axial load or, in this case, the temperature rise. Equilibria are obtained from the first derivative of the potential

$$\frac{dV}{dq} \equiv V'(q) = 4q^3 - 2\lambda q = 0 \quad (2)$$

giving

$$q_{eq} = 0, \pm \sqrt{\frac{\lambda}{2}} \quad (3)$$

The stability of these configurations can be determined by the sign of the second derivative of the potential evaluated at each  $q_{eq}$ :

$$\frac{d^2V}{dq^2} \equiv V''(q) = 12q^2 - 2\lambda \quad (4)$$

The trivial solution is unstable, and the two symmetric solutions are stable.

To consider the generic case, an imperfection parameter must be included. The potential becomes

$$V(q) = q^4 - \lambda q^2 + \epsilon q \quad (5)$$

where  $\epsilon$  might represent an initial geometric imperfection, a small transverse load or an axial load eccentricity. In this case, the symmetry is broken and all three equilibria are nonzero. Physically, one of the stable configurations rep-

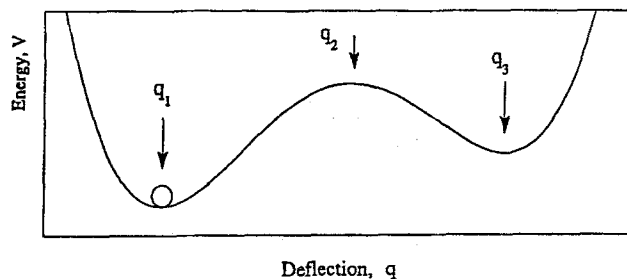


Fig. 2—A schematic of the two-well potential energy function

resents a dominant, primary solution which would be followed by a natural (quasistatic) loading path. The other stable position represents a secondary solution which requires a large perturbation or a special loading history in order to be realized. For small positive values of  $\lambda$ , this “double well” potential is unsymmetric, with one well being deeper than the other.

Figure 2 shows a schematic of this potential energy function for typical parameter values. Furthermore, the deflection of the plate may be conceptually viewed as a ball moving on this potential energy surface.<sup>10</sup> In the static case, the equilibrium configurations and their stability are readily evident. External forcing may be viewed as horizontally shaking the potential surface. For small amplitude excitations, the ball will undergo small periodic oscillations about the primary equilibrium (in the normal course of events). Under greater excitation, the ball may escape the local confines of the potential well and undergo intermittent oscillations as the ball traverses both wells in an unpredictable manner. This motion is the analog to dynamic snap-through of the plate, and the transition between small amplitude, one well motion and the large amplitude snap-through motion forms the basis of the brief experimental study described here.

Another important aspect of this system may be seen in terms of the three amplitude response diagrams of Fig. 3. The nonlinear softening spring and linear and nonlinear hardening spring cases correspond to the curves bending

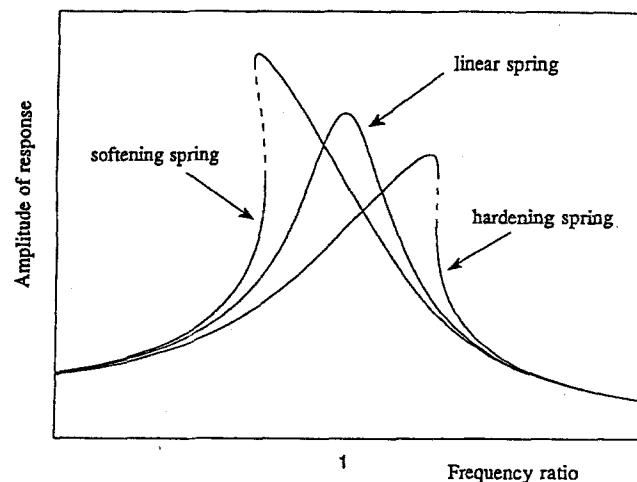


Fig. 3—A schematic amplitude response diagram for motion about a single equilibrium. Softening spring (bending left), linear (straight up) and hardening spring (bending right)

to the left, straight up and bending to the right, respectively.<sup>11</sup> It is important to point out that these diagrams pertain to motion about *one* equilibrium position (*one* potential well). They do not correspond to snap-through amplitudes. Furthermore, for a fixed  $\Delta T < \Delta T_{cr}$ , periodic plate motions are of the hardening type (bending right) due to the additional membrane stiffness. However, in this prebuckled regime the bending stiffness decreases as the thermal load (in-plane load) is increased from ambient to  $\Delta T_{cr}$ . Now consider  $\Delta T > \Delta T_{cr}$ . For a fixed  $\Delta T$ , the system is of the softening spring type (bending left) due to the presence of the unstable equilibrium (the hilltop on the potential surface) separating the two stable equilibria. The bending stiffness in this regime increases with increased thermal load.

## Narrow Band Inputs

### Typical Behavior

Figure 4 shows a small amplitude response about the primary equilibrium for  $\Delta T/\Delta T_{cr} = 1.76$ , with a sound pressure level (SPL) of 140 dB and a frequency of 120 Hz. This response is very nearly linear with a response frequency equal to that of the excitation (see Ref. 1). If the SPL was increased slightly, the motion would still be confined to the one potential well, but the amplitude would grow and demonstrate the typical softening spring characteristics associated with the buckled configuration.

Even for parameter values where small amplitude motion is expected, the transient dynamics play a more significant role due to the possibility of snap-through resulting from disturbances, i.e., perturbations, nonstationary or random effects. For example, consider ramping the excitation level from 130 dB up to 150 dB and then back to 130 dB over a short time interval. The consequences of one such SPL sweep are shown in Fig. 5(a). The response demonstrates a beating phenomenon (occurring between 1 and 1.5 s), which may be connected to a saddle node bifurcation,<sup>12</sup> i.e., the jump in amplitude. This is followed by a burst of tran-

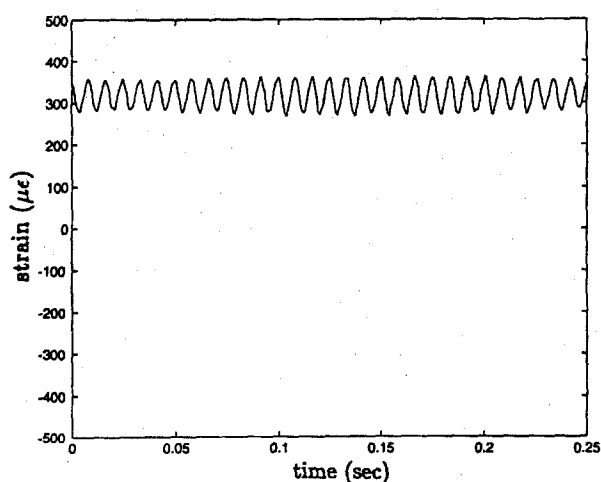


Fig. 4—A small-amplitude, periodic response about the primary equilibrium branch.  $\Delta T/\Delta T_{cr} = 1.76$ , with an SPL of 140 dB and a frequency of 120 Hz

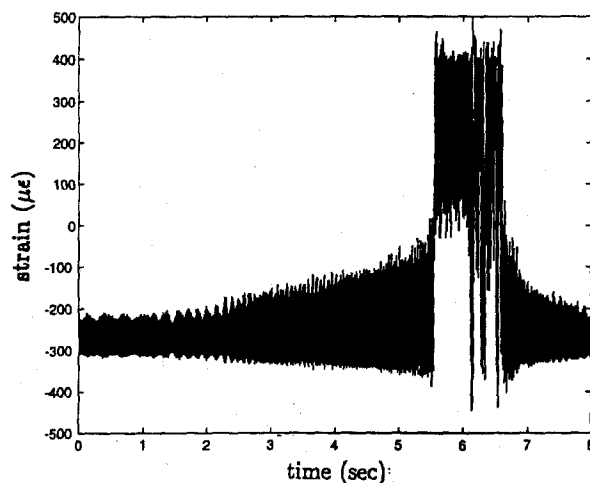
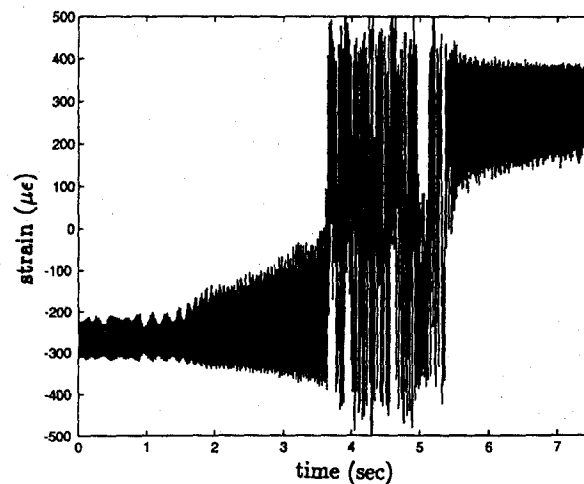


Fig. 5—Transient snap-through responses caused by sweeping the SPL from 130 dB  $\rightarrow$  150 dB  $\rightarrow$  130 dB. (a) The motion began around the secondary equilibrium but then settled around the primary equilibrium. (b) The motion began around the secondary equilibrium and returned there after the burst of transient snap-through

sient cross-well oscillations. When the excitation level is reduced, the system returns to small amplitude motion, but about the other stable equilibrium position. Figure 5(b) shows another test case which produced very different results. Using a similar SPL sweep, the system again experiences a burst of transient snap-through oscillations, but then returns to motion about the original stable equilibrium. This example serves to highlight the fundamental loss of predictability which occurs in nonlinear systems.

In contrast to Figs. 4, 5(a) and 5(b), Fig. 6 shows a steady-state, snap-through oscillation. This response corresponds to  $\Delta T/\Delta T_{cr} = 1.53$ , with an SPL of 155 dB and a frequency of 115 Hz. In spite of having deterministic (non-random) inputs, the motion appears aperiodic. In fact, this highly nonlinear response has been shown to be hyperchaotic,<sup>1</sup> i.e., the oscillation has multiple positive Lyapunov exponents.

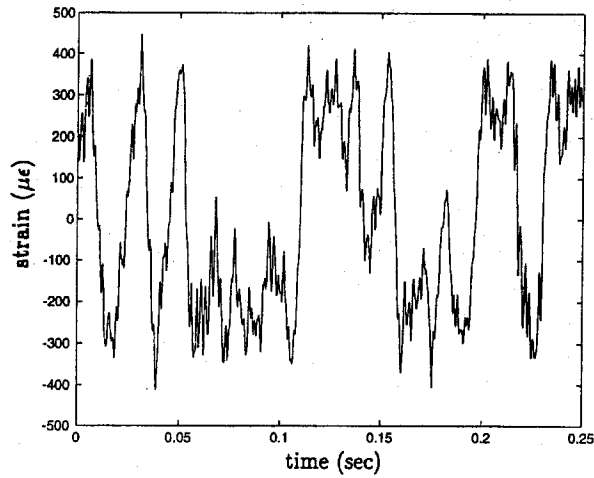


Fig. 6—Steady state snap-through response of the plate.  $\Delta T/\Delta T_{cr} = 1.53$ , with an SPL of 155 dB and a frequency of 115 Hz

### Experimental Procedure

The goal is to identify parameter combinations which result in snap-through oscillations, similar to Fig. 6. However, there are several control parameters to consider. The three most evident are the sound pressure level (SPL), the excitation frequency ( $\omega$ ) and the temperature rise above ambient ( $\Delta T$ ). Rather than looking at this complicated three-dimensional control parameter space, it will prove easier to fix one of the parameters. The obvious choice is  $\Delta T$  because, from static considerations, much is already known about the influence of  $\Delta T$  on snap-through. Figure 7 shows the strain as a function of  $\Delta T$ . For  $\Delta T < \Delta T_{cr}$ , snap-through oscillations are an impossibility because the secondary state has not emerged. Also, at large  $\Delta T$ , the equilibria are sufficiently remote so that snap-through is unlikely. Hence only intermediate ranges of  $\Delta T$  are likely candidates for snap-through. Consequently, the following procedure was carried out to determine regions in the (SPL,  $\omega$ ) plane which result in snap-through near the primary resonance.

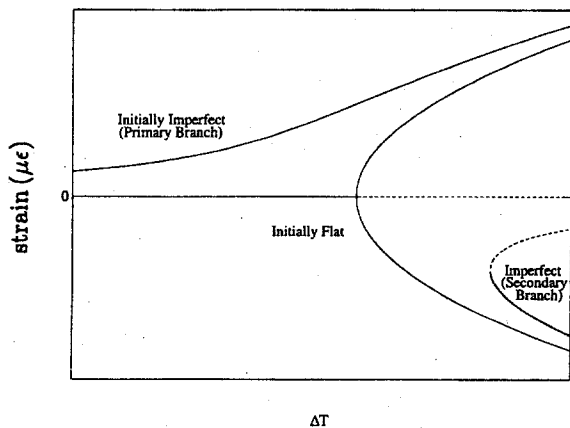


Fig. 7—Schematic of the static equilibrium behavior as a function of temperature rise

The plate is heated to an intermediate temperature in the postcritical (buckled) regime. At that temperature, a low-level broadband acoustic excitation is applied and the plate response is monitored by a spectrum analyzer. From this, the first resonant frequency is easily determined by the frequency response function between the strain and the acoustic input. Due to light damping in the system, this frequency is assumed to be roughly the fundamental natural frequency. The excitation is set at a single frequency below the fundamental, and the SPL is gradually (quasistatically) increased until the system begins to snap through. The combinations of ( $\omega$ , SPL), which result in snap-through, are recorded. The acoustic level is reduced to a low level, and the excitation frequency is incremented. Again, the excitation is slowly increased until the onset of snap-through is found. The corresponding ( $\omega$ , SPL) is recorded. This procedure is carried out at 30 different frequencies near the plate's fundamental frequency.

During a single test at fixed frequency, the dynamic response of the plate is similar in nature to those shown in Figs. 5(a) and 5(b). However, the linear evolution rate of the SPL is much slower, so the inputs are quasistatic, i.e., the time scale involved is much longer.

### Results

For these experiments, the temperature ratio was set at  $\Delta T/\Delta T_{cr} = 1.95$ ; the fundamental natural frequency was found to be 111 Hz. By coincidence, this is the same as the fundamental frequency  $\Delta T = 0$ .

Figure 8 shows the parameter combinations at which snap-through oscillations begin. This boundary clearly separates the parameter space into regions of snap-through and no snap-through. Several observations may be made. First, the lowest excitation required to produce snap-through occurs at a frequency ratio of 0.8. This is well below the linear resonance at a frequency ratio of 1, but is consistent with the softening spring characteristics of the buckled configuration. Second, the boundary is not a straight line or a simple curve. It displays protrusions which are reminiscent of the fractal boundary observed by Virgin and Erickson<sup>13</sup> in their numerical study of another

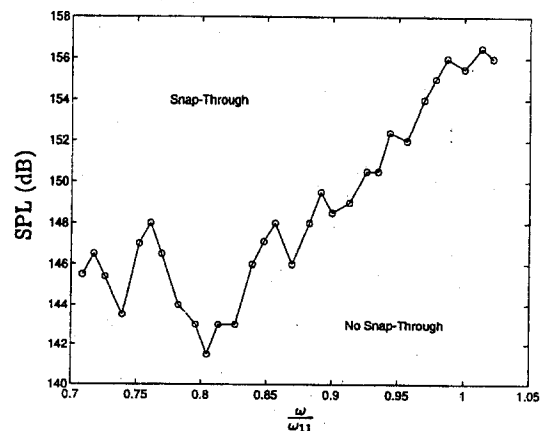


Fig. 8—Snap-through boundary using tonal inputs for  $\Delta T/\Delta T_{cr} = 1.95$

softening spring system. Experimentally, it is impossible to show whether the boundary is fractal due to the limited number of points taken and precision required. Furthermore, determining the onset SPL of steady state snap-through (as opposed to transient snap-through which periodically occurred as the parameters were changed) is subjective. However, it suffices to say that the boundary is nonsmooth and may be fractal.

It is also worth noting that Fig. 8 bears a resemblance to Figs. 4(a) and 4(b) in Ref. 14. In this reference, Dowell and Pezeshki mapped cross-well chaos boundaries for a form of Duffing's equation. Their results showed a similar minimum in the parameter space near a nondimensional forcing frequency of 0.8. These similarities are, perhaps, not surprising in light of the fact that plate systems may be modeled, in certain circumstances, by a set of coupled Duffing oscillators.<sup>1,2,8,9</sup>

## Finite Bandwidth Inputs

### Experimental Procedure

The objective is to determine how the threshold of snap-through is affected by varying the frequency bandwidth of a random acoustic input. As discussed previously, it is reasonable to fix the temperature rise above ambient ( $\Delta T$ ) and consider an input sound pressure level parameter and a frequency parameter. Here, the sound pressure level (SPL) denotes an overall level. The frequency parameter is the center frequency plus the half bandwidth ( $\bar{\omega}$ ). For all cases, the center frequency was chosen to be the first linear natural frequency.

To control the bandwidth of the acoustic excitation, the broadband input signal was passed through a series of four high-pass and four low-pass filters. The efficiency of these filters to limit the bandwidth is measured in terms of the filters' rolloff. The low-pass filters have a cumulative rolloff of 115 dB/octave, while the high-pass filters have a cumulative rolloff of 192 dB/octave.

The system is heated to  $\Delta T/\Delta T_{cr} = 2.0$ . Using a fixed frequency bandwidth, the excitation level is gradually increased, again quasistatically, from a low level until snap-through occurs. The values of ( $\bar{\omega}$ , SPL) are recorded and the bandwidth is widened. This procedure is carried out several times to generate a snap-through boundary.

### Results

The snap-through boundary for the random input is shown in Fig. 9. The overall SPL is plotted against a non-dimensional bandwidth as measured from the center frequency. There is a dramatic drop-off in the boundary as the

frequency parameter  $\frac{\omega_{11} + \bar{\omega}_{11}}{\omega_{11}}$  approaches 1.15 from the

low-bandwidth end. This occurs because the input frequency bandwidth is widening to include (engulf) the nonlinear resonance (see Fig. 3). Recall that Fig. 9 only shows one-half of the frequencies involved, since  $\bar{\omega}$  is the half band-

width. The frequencies  $\frac{\omega_{11} - \bar{\omega}_{11}}{\omega_{11}}$  are also included. This

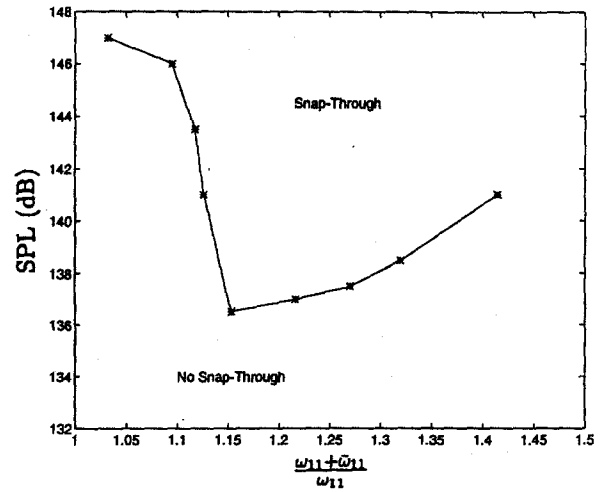


Fig. 9—Effect of bandwidth on the transition to snap-through behavior for  $\Delta T/\Delta T_{cr} = 2.0$

resonance behavior, occurring here around  $\omega/\omega_{11} \approx 0.85$ , makes it easier to snap the plate through. This, in turn, results in a lower SPL needed to cause snap-through.

Finally, although only a few data points are presented in Fig. 9, the boundary is not visibly jagged. It is rather smooth, and there is no suggestion that fractal behavior may be present.

## Discussion

This paper considers the snap-through characteristics of an acoustically excited, thermally loaded, rectangular plate. Rather than focus on the dynamic characteristics of a specific oscillation (see Ref. 1), this paper presents experimental results which identify regions in the control parameter space which result in snap-through.

In the case of tonal (single-frequency) acoustic inputs, the (SPL,  $\omega$ ) plane was viewed at constant temperature ( $\Delta T > \Delta T_{cr}$ ). The boundary separating regions of snap-through and no snap-through dips significantly around  $\omega/\omega_{11} = 0.8$ , which agrees, at least qualitatively, with the softening spring characteristics of the buckled state. Furthermore, the boundary is nonsmooth and possibly contains fractal structure.

Using a random acoustic input, a similar boundary was measured. In this case, the parameter plane was the (SPL,

$\frac{\omega_{11} + \bar{\omega}_{11}}{\omega_{11}}$ ) plane, where  $\bar{\omega}_{11}$  is the half bandwidth. As the

bandwidth is widened from the center frequency, the SPL required to cause snap-through decreases to a minimum

around  $\frac{\omega_{11} + \bar{\omega}_{11}}{\omega_{11}} = 1.15$ . This occurs because the non-

linear resonance frequencies are being included in the excitation ( $\omega/\omega_{11} \approx 0.85$ ). However, this boundary is relatively smooth and does not show any evidence that fractal behavior may exist.

## Acknowledgment

This work was partially supported by the Structural Acoustics Branch of the NASA Langley Research Center through NASA GSRP Grant No. NGT-50989.

## References

1. Murphy, K.D., Virgin, L.N. and Rizzi, S.A., "Characterizing the Dynamic Response of Pre- and Post-critical Plates Subject to Elevated Temperatures and Acoustic Excitation," *J. Sound and Vibration*, forthcoming.
2. Dowell, E.H., "Flutter of a Buckled Plate as an Example of Chaotic Motion of a Deterministic Autonomous System," *J. Sound and Vibration*, **85** (3), 195-204 (1985).
3. Ng, C.F., "Nonlinear and Snap-through Response of Curved Panels to Intense Acoustic Excitation," *J. Aircraft*, **26** (3), 281-288 (1989).
4. Ng, C.F. and Clevenson, S.A., "High-intensity Acoustic Tests of a Thermally Stressed Plate," *J. Aircraft*, **28** (4), 275-281 (1989).
5. Tseng, W.T. and Dugundji, J., "Nonlinear Vibrations of a Buckled Beam under Harmonic Excitation," *J. Appl. Mech.*, **38**, 467-476 (1971).
6. Thompson, J.M.T. and Hunt, G.W., *Elastic Instability Phenomena*, John Wiley & Sons, Chichester, England (1984).
7. Clevenson, S.A. and Daniels, E.F., "Capabilities of the Thermal Acoustic Fatigue Apparatus," NASA Technical Memorandum 104106 (1992).
8. Murphy, K.D., Virgin, L.N. and Rizzi, S.A., "The Effect of Thermal Prestress on the Free Vibration Characteristics of Clamped Rectangular Plates: Theory and Experiment," *J. Vibration and Acoustics*, forthcoming.
9. Murphy, K.D., "Theoretical and Experimental Studies in Nonlinear Dynamics and Stability of Elastic Structures," PhD diss., Duke University, Durham, NC (1994).
10. Gottwald, J.A., Virgin, L.N. and Dowell, E.H., "Experimental Mimicry of Duffing's Equation," *J. Sound and Vibration*, **158** (3), 447-467 (1992).
11. Jordan, D.W. and Smith, P., *Nonlinear Ordinary Differential Equations*, Oxford University Press, New York (1987).
12. Thompson, J.M.T. and Virgin, L.N., "Predicting a Jump to Resonance Using Transient Maps and Beats," *Int. J. Non-linear Mech.*, **21** (3), 205-216 (1986).
13. Virgin, L.N. and Erickson, B.K., "A New Approach to Overturning Stability of Floating Structures," *Ocean Eng.*, **21** (1), 67-80 (1994).
14. Dowell, E.H. and Pezeshki, C., "On the Understanding of Chaos in Duffings Equation Including a Comparison with Experiment," *J. Appl. Mech.*, **53** (1), 5-9 (1986).